



HAL
open science

Using extrapolation techniques in VOF methodology to model expanding bubbles

L.C. Malan, R Scardovelli, Stéphane Zaleski

► **To cite this version:**

L.C. Malan, R Scardovelli, Stéphane Zaleski. Using extrapolation techniques in VOF methodology to model expanding bubbles. *Procedia IUTAM*, 2015, 15, pp.228-235. 10.1016/j.piutam.2015.04.031 . hal-01158526

HAL Id: hal-01158526

<https://hal.sorbonne-universite.fr/hal-01158526>

Submitted on 1 Jun 2015

HAL is a multi-disciplinary open access archive for the deposit and dissemination of scientific research documents, whether they are published or not. The documents may come from teaching and research institutions in France or abroad, or from public or private research centers.

L'archive ouverte pluridisciplinaire **HAL**, est destinée au dépôt et à la diffusion de documents scientifiques de niveau recherche, publiés ou non, émanant des établissements d'enseignement et de recherche français ou étrangers, des laboratoires publics ou privés.



Distributed under a Creative Commons Attribution - NonCommercial - NoDerivatives 4.0 International License



IUTAM Symposium on Multiphase flows with phase change: challenges and opportunities,
Hyderabad, India (December 08 – December 11, 2014)

Using extrapolation techniques in VOF methodology to model expanding bubbles

L.C. Malan^{a,b}, R. Scardovelli^c, S. Zaleski^{a,b,*}

^a*Sorbonne Universités, UPMC Univ Paris 06, UMR 7190, Institut Jean le Rond d'Alembert, F-75005, Paris, France*

^b*CNRS, UMR 7190, Institut Jean le Rond d'Alembert, F-75005, Paris, France*

^c*DIN-Laboratorio di Montecuccolino, Università di Bologna, Via dei Colli 16, 40136 Bologna, Italy*

Abstract

A numerical method is presented to study cavity and bubble dynamics. The liquid phase is assumed to be inviscid and incompressible and separated from the gas or vacuum phase by a free surface. On the free surface the stress tensor reduces to a spatially constant pressure. The flow in the bulk of the liquid is computed using a second-order-in-time projection method. The interface is advected and reconstructed using a Volume-of-Fluid (VOF) method. Setting the pressure on the free surface to the prescribed value involves a modified stencil on nodes close to the interface. This modified stencil contains interpolated pressures on branches that are cut by the interface. Capillary effects are taken into account by adding the Laplace law pressure increment to these prescribed pressures. The curvature that appears in the Laplace law is computed using the height-function method. The VOF advection and momentum advection schemes both require an extension of the velocity in a two-layer wide ghost cell region on the grid across the free surface. This ghost layer is computed in two stages. In the preliminary stage a first-order velocity extrapolation of the liquid velocity field to the ghost layers is performed. In the second stage the ghost layer velocities are projected on the space of divergence free velocities using an auxiliary projection step. The whole procedure is implemented in a free code developed with the help of Gretar Tryggvason and Yue (Stanley) Ling and is available at <http://parissimulator.sf.net>.

Tests are performed on radial flows with spherical symmetry except for boundary conditions far from the bubble in a cubic box. In such a geometry the flow is predicted by solutions of the Rayleigh-Plesset equation. Good comparison to the Rayleigh-Plesset solution for a single bubble with low and moderate amplitude oscillations is shown. Perspectives for parallel simulations involving very large numbers of bubbles are given.

© 2015 The Authors. Published by Elsevier B.V. This is an open access article under the CC BY-NC-ND license (<http://creativecommons.org/licenses/by-nc-nd/4.0/>).

Peer-review under responsibility of Indian Institute of Technology, Hyderabad.

Keywords: Free surfaces, Volume-of-fluid, bubbles, cavitation

1. Introduction

Numerical simulation of two-phase flows has a large scientific interest with many industrial applications. Various interface tracking methods using the so-called “one-fluid” approach and an incompressible fluid model have been

* Corresponding author. Tel.: +33-000-000-0000 ; fax: +0-000-000-0000.

E-mail address: zaleski@dalembert.upmc.fr

developed to study these flows. Furthermore, two-fluid flow problems often can be reduced to free-surface flows which require accurate boundary conditions on the interface. The study of free-surface flows was pioneered by Harlow and Welch¹ with the development of the Marker-and-Cell (MAC) method. It has also been implemented in the volume-of-fluid (VOF) framework^{2,3} to simulate flows with interfaces where one phase is a light gas. Since then it has been used to study natural flows, such as water waves^{4,5}, and industrial devices, such as inkjet printing^{6,7}. Bubble dynamics and cavitation are also active research areas that can be attacked with the VOF method. Other approaches include the front tracking method, as in the study by Popinet⁸ of the effect of viscosity in near-wall bubble, and the level set method, as in the study by Can and Prosperetti⁹ of vapor bubble dynamics. A review of these methods have been published by Scardovelli and Zaleski¹⁰ and later with the addition of Tryggvason¹¹.

This paper will describe a VOF method that is used to simulate bubble dynamics with a free-surface approach. VOF methods have been improved significantly since their introduction by Hirt and Nichols². Important contributions include the reconstruction of the interface using piece-wise linear elements (PLIC)¹², momentum-conserving schemes¹³ and height functions^{14,15,16,17,18} to calculate local geometrical quantities such as interface normal and curvature. Interface advection to conserve mass to machine accuracy has also been achieved by Weymouth and Yue¹⁹.

2. Problem formulation

The problem considers two fluid phases separated by an arbitrary, moving interface. In the present study we assume an adiabatic flow with no mass transfer across the interface. The focus is on a low Mach number flow, that allows us to use an incompressible formulation of the momentum equation. The gas phase is a few orders of magnitude lighter than the liquid, therefore we can assume a free-surface flow with appropriate boundary conditions on the interface. Furthermore, we neglect viscous effects as the liquid flow is characterized by very high Reynolds numbers. This leads to a fluid system governed by the incompressible Euler equations:

$$\rho \left(\frac{\partial \mathbf{u}}{\partial t} + \mathbf{u} \cdot \nabla \mathbf{u} \right) = -\nabla P, \quad (1)$$

$$\nabla \cdot \mathbf{u} = 0,$$

where $\mathbf{u} = (u, v, w)$ is the fluid velocity, $\rho = \rho_l$ its density, and P the pressure. With the free surface interface condition, the pressure on the interface is given by

$$P_I = P_0 - \sigma \kappa, \quad (2)$$

where σ is the surface tension coefficient, κ the local interface curvature and P_0 the gas or cavity pressure which is assumed to be constant in space. P_I is the interface pressure, on the liquid side of the interface. Note that since we assume zero viscosity, we do not have to enforce a shear-free condition on the interface. The interface is tracked using a volume-of-fluid² approach, that considers a *colour* function, C , that obeys a standard advection equation:

$$\frac{\partial C}{\partial t} + \nabla \cdot (C \mathbf{u}) = 0. \quad (3)$$

The function C represents the volume fraction of a reference phase present in the spatial domain. Here we choose the gas as the reference phase, therefore for an arbitrary volume V the value of C is given by

$$C = 1 - \frac{1}{\rho_l V} \int_V \rho(x, y, z) dV, \quad (4)$$

where ρ_l is the constant liquid density. We recall that in the free surface approach the gas density ρ_g is equal to zero.

3. Numerical formulation for bubble dynamics problem

To solve this problem numerically, we consider a projection method originally developed in²¹ and also used in^{8,16}. The method has been implemented in the numerical code PARIS, which is an acronym for PARallel Robust Interface Simulator, and it is freely available under the GPL license agreement. The projection method solves the system of

equations in (1) by first calculating a provisional velocity field \mathbf{u}^* . This field is obtained by integrating all momentum contributions with the exception of the pressure P :

$$\frac{\mathbf{u}^* - \mathbf{u}^n}{\Delta t} = -\mathbf{u}^n \cdot \nabla_h \mathbf{u}^n, \quad (5)$$

where ∇_h is the discrete gradient operator. The superscript n refers to the n^{th} time step of length Δt . The velocity at the next time $n + 1$ is then obtained by adding the pressure contribution to the provisional velocity \mathbf{u}^*

$$\frac{\mathbf{u}^{n+1} - \mathbf{u}^*}{\Delta t} = -\frac{1}{\rho^*} \nabla_h P^*, \quad (6)$$

where ρ^* is the interpolated density across the staggered grid. The sum of equations (5) and (6) gives the discrete form of the momentum equation, (1). To ensure mass conservation, we must have

$$\nabla_h \cdot \mathbf{u}^{n+1} = 0. \quad (7)$$

By taking the divergence of (6) we obtain a Poisson equation for the pressure

$$\nabla_h \cdot \left(\frac{\Delta t}{\rho^*} \nabla_h P^* \right) = \nabla_h \cdot \mathbf{u}^*. \quad (8)$$

The projection method is used in combination with a second-order Runge-Kutta time integration to solve system (1). The method becomes second-order in time by averaging two explicit, first-order steps. The sequence of integration steps is the following:

1. a provisional velocity field \mathbf{u}^* is obtained by solving (5)

$$\frac{\mathbf{u}^* - \mathbf{u}^n}{\Delta t} = -\mathbf{u}^n \cdot \nabla_h \mathbf{u}^n,$$

2. the pressure field P is obtained by solving (8)

$$\nabla_h \cdot \left(\frac{\Delta t}{\rho^*} \nabla_h P^* \right) = \nabla_h \cdot \mathbf{u}^*,$$

3. an intermediate velocity field \mathbf{u}' is then obtained by correcting \mathbf{u}^* as given by (6)

$$\frac{\mathbf{u}' - \mathbf{u}^*}{\Delta t} = -\frac{1}{\rho^*} \nabla_h P^*,$$

4. steps 1-3 are repeated with another explicit time step, starting from the previously calculated values at the intermediate level

$$\begin{aligned} \frac{\mathbf{u}^{**} - \mathbf{u}'}{\Delta t} &= -\mathbf{u}' \cdot \nabla_h \mathbf{u}' \\ \nabla_h \cdot \left(\frac{\Delta t}{\rho^{**}} \nabla_h P^{**} \right) &= \nabla_h \cdot \mathbf{u}^{**} \\ \frac{\mathbf{u}'' - \mathbf{u}^{**}}{\Delta t} &= -\frac{1}{\rho^{**}} \nabla_h P^{**} \end{aligned}$$

We then obtain a second-order approximation to the velocity field at time step $n + 1$ by averaging

$$\mathbf{u}^{n+1} = \frac{1}{2} (\mathbf{u}'' + \mathbf{u}^n) \quad (9)$$

3.1. Pressure treatment at the free surface

For the pressure we need to solve the Poisson equation, (8), with Dirichlet’s boundary conditions that on the interface are derived from (2). In the computational domain there are three different types of cells: cells with only the reference gas phase, where the *colour* function $C = 1$, cells with only the liquid phase, and $C = 0$, and cells cut by the interface, with $0 \leq C \leq 1$. In the cut cells the interface is reconstructed with a Piecewise Linear Interface Calculation (PLIC), from the idea of DeBar¹². This means that the interface is reconstructed by using a portion of a plane in every cut cell.

In the Marker-and-Cell (MAC) method the discrete pressure is located at the center of the grid cell. It is then straightforward to show that all pressure nodes inside a cell with a value of the colour function greater than 0.5 will be located inside the gas phase. These cells are not considered in the solution of the Poisson’s equation and only the appropriate pressure boundary condition is applied on the interface. The pressure value P_I on the liquid side of the interface is then given by (2)

$$P_I = P_0 - \sigma \kappa \tag{10}$$

This condition is applied on the interface by using a modified finite difference pressure gradient operator, as suggested by Chan and Street⁴, while solving (8) for the pressure in the projection step. To explain the modification, consider the finite difference pressure in the x -direction, as shown in Fig. 1. The component of the pressure gradient along the

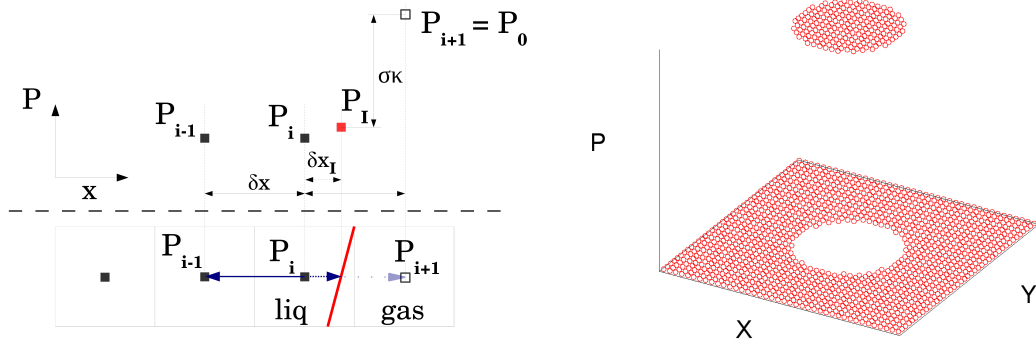


Fig. 1. On the left a 1D schematic image illustrates the modification of the pressure discretisation for the free surface approach. Surface tension is included by adding the Laplace pressure jump at the interface. On the right the image shows the pressure field inside and around a single 2D bubble to illustrate the discontinuous change in the pressure value across the interface.

x -direction with centered finite differences is given by the standard expression

$$\nabla_h P_{i+1/2} = \frac{P_{i+1} - P_i}{\delta x}, \tag{11}$$

where δx is the distance between two consecutive pressure nodes along the x -direction. This operator needs to be modified across the interface in order to apply the Dirichlet’s boundary condition on the pressure at the interface

$$\nabla_h P_{i+1/2} = \frac{P_I - P_i}{\delta x_I} \tag{12}$$

where δx_I is the distance between the pressure node under consideration and the interface along the x -direction, as shown in figure 1, while P_I is the pressure on the interface given by (10). In order to apply this modification both the interface location and the local curvature κ are needed.

The curvature value is computed in all cut cells through the evaluation of the height function¹⁵, in a way similar to that used in other codes, such as Gerris¹⁷. To determine the interface location and more specifically to calculate the modified distance δx_I , however, we have developed a new, original approach. In particular, we need to determine

all liquid nodes for which the finite difference approximation of the pressure gradient needs to be modified. To this aim we consider a topological approach, where all pressure nodes are labelled either as liquid or as gas. We then consider any cell of the computational domain which is a liquid node. If one of the six neighbouring cells, sharing a face with the given cell, is a gas node, we compute the modified distance along the coordinate direction to the gas node. This distance is found by considering a VOF reconstruction in a staggered cell between the two pressure nodes with a different label. On the left of figure 1 the 2D staggered cell is that comprised between the liquid node P_i and the gas node P_{i+1} .

For the interface reconstruction it is necessary to compute the interface normal vector \mathbf{m} and the planar interface is then given by the expression^{11,22}

$$\mathbf{m} \cdot \mathbf{x} = m_x x + m_y y + m_z z = \alpha \quad (13)$$

where the plane constant α is directly related to the value of the colour function C . The VOF fraction in a staggered cell is calculated from the existing reconstructions in the two consecutive liquid and gas cells, by adding the VOF fraction of the two neighbouring half cells. The interface normal in the staggered cell is used by calculating a weighted average of the normals in the liquid and gas cells in between which the modified distance, δx_l is required.

$$\mathbf{m}' = \mathbf{m}_l \frac{C_l}{C_l + C_g} + \mathbf{m}_g \frac{C_g}{C_l + C_g}, \quad (14)$$

where \mathbf{m}' , \mathbf{m}_l and \mathbf{m}_g are the respective interface normals in the staggered, liquid and gas cells. C_l and C_g are the respective VOF fractions in the liquid and gas cells. Figure 2 illustrates the VOF reconstruction in a staggered cell in

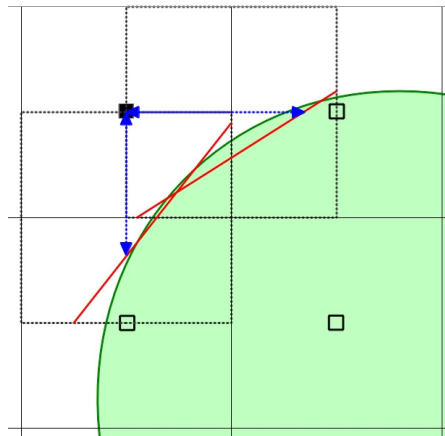


Fig. 2. The modified finite difference lengths are found by using a VOF reconstruction in staggered cells.

between the liquid-gas pressure node pair. In this example a liquid node has gas neighbours to the right and below.

3.2. Velocity extrapolation

In this section we discuss the treatment of the velocity at the interface. Since we are assuming a liquid phase with no viscosity, the interface will always be shear free. However, in the numerical discretization of the advection term in the momentum equation, $\mathbf{u} \cdot \nabla \mathbf{u}$, we require up to two neighbouring velocity values to correctly calculate the momentum contribution of the liquid velocity at the interface boundary. These additional points can be viewed as ghost values which are required to implement the boundary condition. However, the momentum equation is neglected inside the gas phase, therefore it is necessary to find these ghost velocities by extrapolating the velocity field computed inside the liquid phase.

In the Marker-and-Cell (MAC) grid the velocity components are located on the cell faces, each component located on the face with the normal parallel to the corresponding coordinate direction. Each velocity component is also positioned between two consecutive pressure nodes. The same topological approach that was used for the pressure

nodes is used for the velocity components, in particular to determine if that component is computed by the solution of the momentum equation or found by an extrapolation. In this case, if a velocity component is on a cell face of a liquid node, then it will be computed directly by solving the Euler equations. This is also true for the velocity components lying between a liquid and a gas node, since in the projection method the modified pressure gradient of equation (12) will be used in (6) to correct the provisional velocity. However, the velocity components in between two gas pressure nodes are not directly computed and their value needs to be extrapolated from the neighbouring resolved components. Figure 3 shows an image of a numerical grid with the position of the scalar variables and vector components. The extrapolation is performed after the correction of the provisional velocity field, independently for

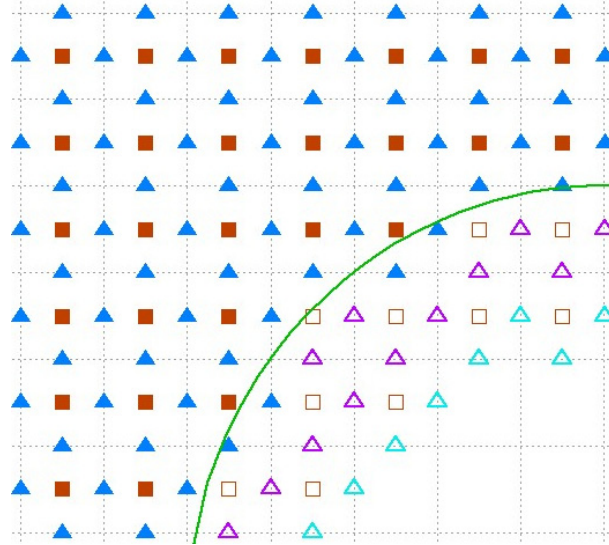


Fig. 3. The image shows the numerical grid in a 2D section of a bubble. The green line is the actual interface, calculated values of the pressure and velocity components are represented by full markers, and extrapolated values by empty markers.

each scalar component. The extrapolation is first-order accurate and it is given by the average value of all closest liquid neighbours. The procedure can be easily extended to second-order by using a least-square fit of neighbouring velocities⁸.

Ensuring volume conservation

After the two layers of velocity components inside the gas phase have been computed by extrapolation, an additional step is required to ensure that the extrapolated velocities are discretely divergence-free. This further step is necessary, because the extrapolated velocities inside the gas phase near the interface are used to advect the interface, as implied by 3. If these discrete velocities are not divergence-free, volume conservation will not be enforced. The divergence-free condition is enforced by considering a second projection step, where only the first two layers of cells inside the gas phase are involved, and all other cells remains unchanged. As in the projection step previously illustrated, a “phantom” pressure is obtained in these two layers

$$\nabla_h \cdot (\nabla_h \hat{P}) = \nabla_h \cdot \tilde{\mathbf{u}}, \quad (15)$$

where \hat{P} is the phantom pressure and $\tilde{\mathbf{u}}$ the extrapolated velocity in the two layers inside the gas phase. This auxiliary pressure field is only calculated to correct the divergence of the extrapolated velocity field. The extrapolated velocity field is then corrected by the pressure gradient

$$\tilde{\mathbf{u}}^{n+1} = \tilde{\mathbf{u}} - \nabla_h \hat{P} \quad (16)$$

4. Numerical tests

A classical test is to compare a simulation of a single gas bubble with a fixed liquid pressure at infinity to the solution of the Rayleigh-Plesset equation²³. This equation describes the evolution of a bubble of radius R in an incompressible liquid, assuming spherical symmetry with a fixed pressure at infinity. Without viscosity, we have:

$$\begin{aligned} \ddot{R}R + \frac{3}{2}\dot{R}^2 &= \frac{P_R - P_\infty}{\rho_l} \\ &= \frac{P_c - \frac{2\sigma}{R} - P_\infty}{\rho_l} \end{aligned} \quad (17)$$

with R the bubble radius, P_R the pressure on the liquid side of the interface and P_∞ the pressure at infinity. σ is the surface tension and ρ_l the liquid density. A bubble of initial radius 0.10 is placed in a liquid with density 1.0 and a surface tension of 0.10. The bubble's reference pressure is 1.0 with an equilibrium radius of 0.09. We set the pressure at infinity at 0.5. The bubble pressure, P_c is obtained from a polytropic gas law.

$$P_c = P_{eq} \left(\frac{R_{eq}}{R} \right)^{3\gamma} \quad (18)$$

with P_{eq} and R_{eq} the respective equilibrium pressure and radius of the bubble. γ is the isentropic gas coefficient. The domain used for the simulation is a cube of size 1.0, with the bubble placed exactly at its center. In order to apply a Dirichlet boundary condition for the pressure, we solve the Rayleigh-Plesset equation (17) numerically at every time step in PARIS using a 5th order Runge-Kutta integration method. The result of this equation is used to determine the pressure at a finite radius, r , which is used to set the pressure at the boundary.

$$P(r, t) = P_R - \rho_l \left(\frac{\dot{R}^2 R^4}{2r^4} - \frac{\ddot{R}R^2 + 2RR\dot{R}^2}{r} + \ddot{R}R + \frac{3}{2}\dot{R}^2 \right) \quad (19)$$

Figure 4 shows a comparison between the results in PARIS and a numerical solution of the Rayleigh-Plesset equation. A slight overestimation of the bubble growth is perceived, which is compounded over consecutive cycles. The general

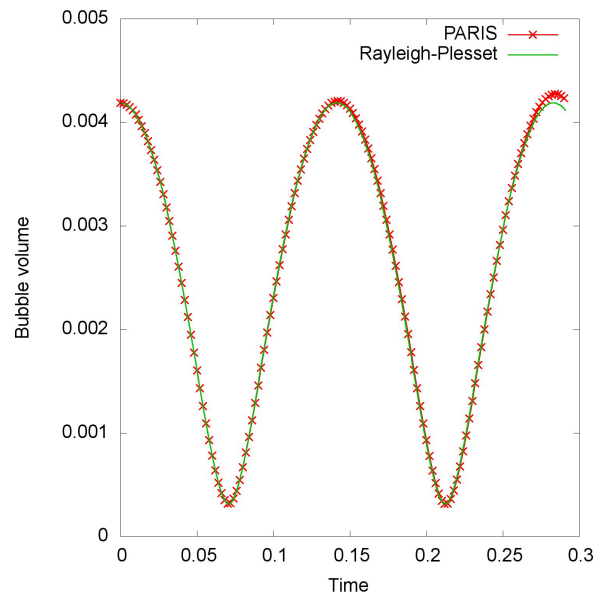


Fig. 4. Comparison of results of a single oscillating gas bubble simulated by PARIS and the Rayleigh-Plesset equation.

comparison is good and encouraging for further bubble dynamics studies.

5. Conclusion

A numerical method to study cavity and bubble dynamics has been presented. The pressure on the free surface is set using a modified stencil with a sharp implementation for surface tension. The topological approach used makes the code well-suited for large scale simulations of bubble clusters to obtain statistical representative results of bubble interactions. Further investigation into different momentum advection schemes is ongoing. The effect of using a second instead of first order velocity extrapolation will also be considered.

References

1. Harlow FH, Welch JE. Numerical Calculation of Time-Dependent Viscous Incompressible] Flow of Fluid with Free Surface. *Phys. Fluid* 1965; **8**:2182-2189.
2. Hirt CW, Nichols BD. Volume of Fluid (VOF) Method for the Dynamics of Free Boundaries. *J. Comput. Phys.* 1981; **39**:201-225.
3. Nichols BD and Hirt CW: Improved free surface boundary conditions for numerical incompressible-flow calculations. *J. Comput. Phys.* 1971; **8**:434-448.
4. Chan RK-C, Street RL. A Computer Study of Finite-Amplitude Water Waves. *J. Comput. Phys.* 1970; **6**:68-94.
5. LeVeque RJ, Shyue K-M: Two-Dimensional Front Tracking Based on High Resolution Wave Propagation Methods. *J. Comput. Phys.* 1996; **123**:354-368.
6. Liou TM, Shih KC, Chau SW, Chen SC: Three Dimensional Simulations of the Droplet Formation During the Inkjet Printing Process. *Int. Comm. Heat Mass Transfer* 2002 vol. 29 **8**:1109-1118.
7. Wu H-C, Hwang W-S, Lin H-J: Development of a three-dimensional simulation system for micro-inkjet and its experimental verification. *Materials Science and Engineering A* 2004; **373**:268-278
8. Popinet S, Zaleski S. Bubble collapse near a solid boundary: a numerical study of the influence of viscosity. *J. Fluid Mech.* 2002; **464**:137-163
9. Can E, Prosperetti, A. A level set method for vapor bubble dynamics. *J. Comput. Phys.* 2012; **231**:1533-1552.
10. Scardovelli R, Zaleski S: Direct Numerical Simulations of Free-Surface and Interfacial Flow. *Annu. Rev. Fluid Mech.* 1999; **31**:567-603.
11. Tryggvason G, Scardovelli R, Zaleski S: *Direct Numerical Simulations of Gas-Liquid Multiphase Flows*. New York: Cambridge University Press; 2011.
12. DeBar R: Fundamentals of the KRAKEN code. *Tech. rep. UCIR-760*. 1974; Lawrence Livermore Nat. Lab.
13. Rudman, M: A Volume-Tracking Method for Incompressible Multifluid Flows with Large Density Variations. *Int. J. Numer. Meth. Fluids* 1998; **28**:357-378.
14. Nichols BD, Hirt CW: Calculating three-dimensional free surface flows in the vicinity of submerged and exposed structures. *J. Comput. Phys.* 1973; **12**:234-246.
15. Torrey M, Cloutman L, Mjolsness R, Hirt C: NASA-VOF2D: a computer program for incompressible flows with free surfaces. *Tech. rep.* 1985; Los Alamos National Laboratory.
16. Sussman M: A second order coupled level set and volume-of-fluid method for computing growth and collapse of vapor bubbles. *J. Comput. Phys.* 2003; **187**:110-136.
17. Popinet S: An accurate adaptive solver for surface-tension-driven interfacial flows. *J. Comput. Phys.* 2009; **228(16)**:5838-5866.
18. Bornia G, Cervone A, Manservigi S, Scardovelli R, Zaleski S: On the properties and limitations of the height function method in two-dimensional Cartesian geometry. *J. Comput. Phys.* 2011; **230(4)**:851-862.
19. Weymouth GD, Yue DK-P: Conservative Volume-of-Fluid Method for Free-Surface Simulations on Cartesian-grids. *J. Comput. Phys.* 2010; **229**:2853-2865.
20. Harlow FH, Welsch JE: The MAC Method: A Computing Technique for Solving Viscous, Incompressible, Transient Fluid Flow Problems Involving Free Surfaces. *Los Alamos Scientific Laboratory report* 1966; LA-3425.
21. Chorin A: On the convergence of discrete approximations to the Navier-Stokes equations. *Mathematics of Computation* 1969; **23(106)**:341-353.
22. Scardovelli R, Zaleski S: Interface reconstruction with least-square fit and split Lagrangian-Eulerian advection. *Int. J. Num. Methods in Fluids* 2003; **41**:251-274.
23. Plesset MS, Prosperetti A: Bubble dynamics and cavitation. *Annu. Rev. Fluid Mech.* 1977; **9**:145-185.